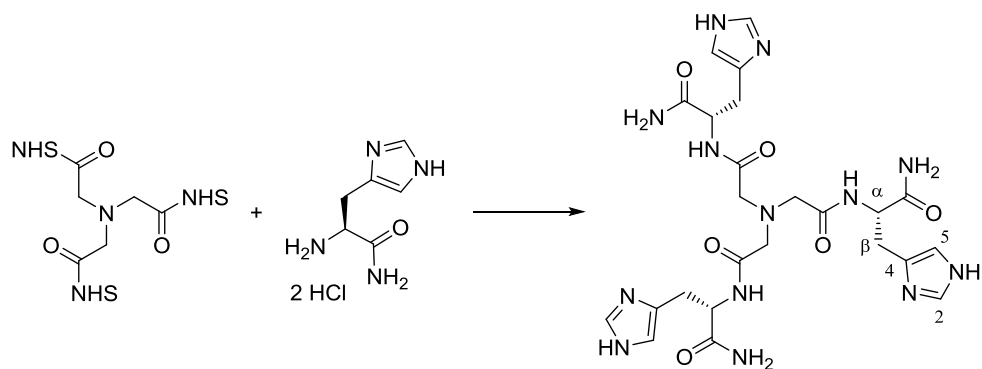


# Supporting Information

## Content

<b>Scheme S1.</b> Synthesis of <b>L</b>	<b>p S2</b>
<b>Figure S1.</b> (+)ESI-MS spectrum of the Cu <sup>II</sup> <b>L</b> complex.	p S2
<b>Figure S2.</b> EPR signatures of Cu <sup>II</sup> <b>L</b> at different pH values.	p S3
<b>Figure S3.</b> (+)ESI-MS spectrum of the Cu <sup>I</sup> <b>L</b> complex.	p S3
<b>Figure S4.</b> EXAFS data for the Cu <sup>I</sup> <b>L</b> complex.	p S4
<b>Figure S5.</b> Cyclic voltamograms of O <sub>2</sub> and ascorbate	p S5
<b>Figure S6.</b> EPR competition between Cu <sup>II</sup> Aβ <sub>1-16</sub> and <b>L</b> . Linear combinations.	p S5
<b>Figure S7.</b> XANES competition between Cu <sup>I</sup> Aβ <sub>1-16</sub> and <b>L</b> . Linear combinations.	p S6
<b>Figure S8.</b> Kinetics of ascorbate consumption with peptide Aβ <sub>1-16</sub> .	p S7
<b>Figure S9.</b> Fluorescence kinetics of CCA experiments	p S8
<b>Figure S10.</b> 400 MHz <sup>1</sup> H NMR spectrum in D <sub>2</sub> O at 300 K.	p S9
<b>Figure S11.</b> 100 MHz <sup>13</sup> C NMR spectrum decoupled from <sup>1</sup> H in D <sub>2</sub> O at 300 K.	P S10



**Scheme S1.** Synthesis of  $L \approx \text{NTA}(\text{HisNH}_2)_3$  – reagents and conditions: DIEA,  $\text{CH}_3\text{CN}/\text{DMF}$ , 11 %

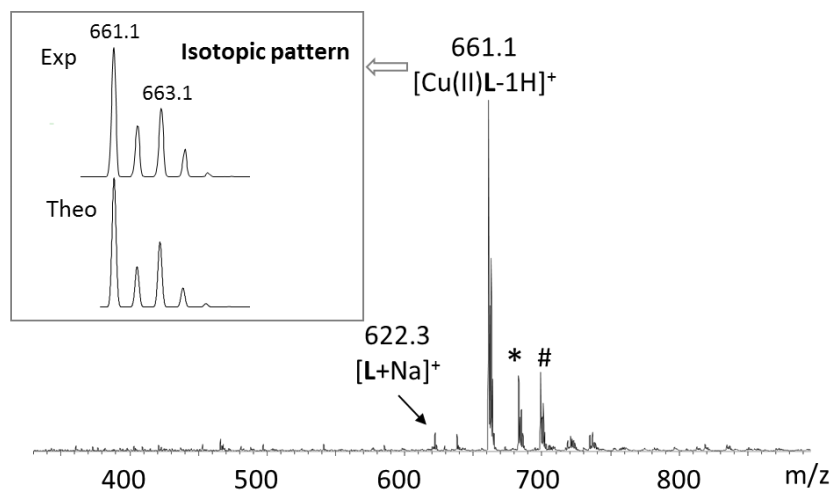


**Figure S1.** (+)ESI-MS spectrum of  $L$  (100  $\mu\text{M}$ ) with equimolar  $\text{Cu}^{\text{II}}\text{SO}_4$ , in ammonium acetate buffer (20 mM, pH 6.9). \* Sodium adducts. # Potassium adducts.

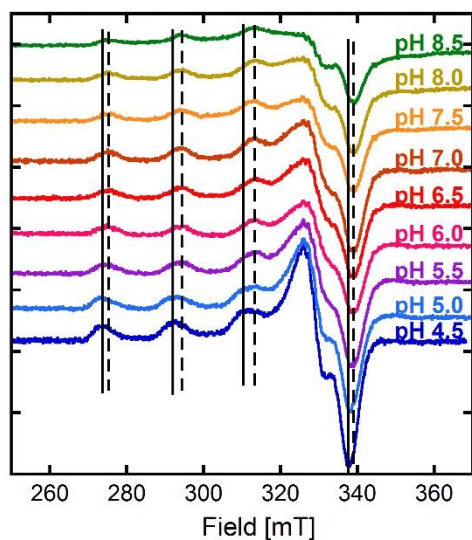


**Figure S2.** EPR signatures of  $\text{Cu}^{\text{II}}\text{L}$  at different pH values.  $[\text{L}] = 200 \mu\text{M}$ ,  $[\text{Cu}^{\text{II}}] = 180 \mu\text{M}$ . 10% of glycerol was used as cryoprotectant.  $T = 110 \text{ K}$ .

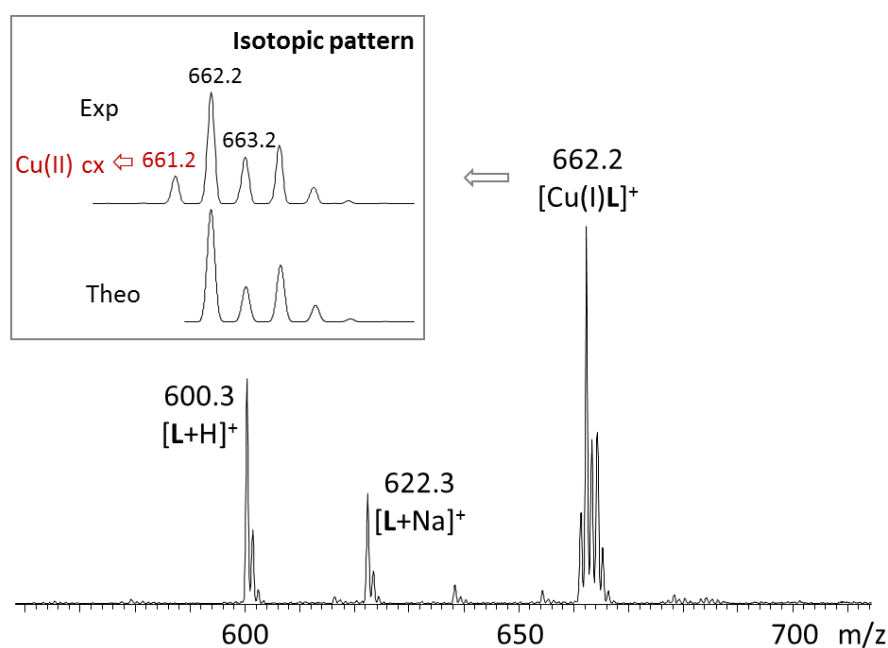


**Figure S3.** (+)ESI-MS spectrum of  $\text{L}$  ( $100 \mu\text{M}$ ) with equimolar  $\text{Cu}^{\text{I}}(\text{CH}_3\text{CN})_4\text{PF}_6$ , in ammonium acetate buffer ( $20 \text{ mM}$ ,  $\text{pH } 6.9$ ).

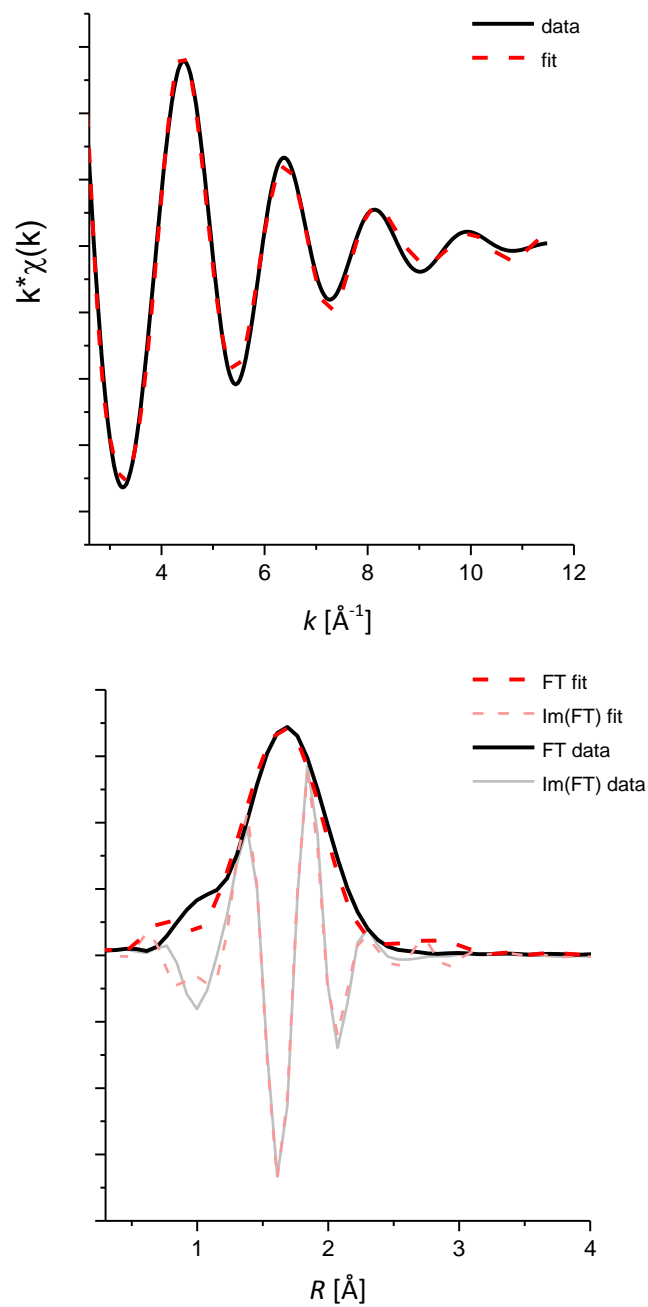


**Figure S4.** EXAFS data for the Cu<sup>I</sup>L complex. Top. Experimental data (solid black curve) and simulated fit (dotted red line) of the filtered first shell of the EXAFS function and Down. the corresponding radial structure functions (RSF, not corrected phase shift). FT and Im(FT) are the magnitude and imaginary part of Fourier transforms, respectively.

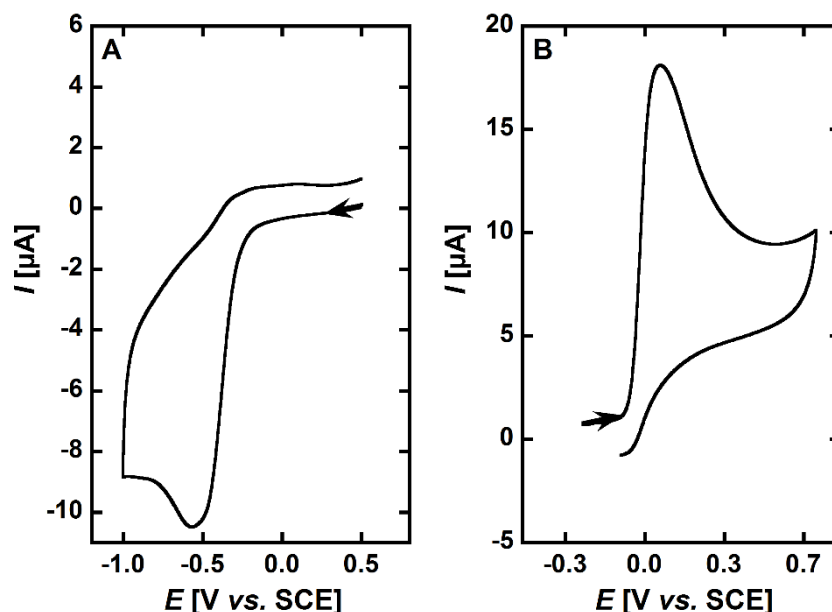


**Figure S5.** Cyclic voltamograms of  $O_2$  (*Panel A*) and ascorbate (*Panel B*).  $[O_2] = \sim 0.2$  mM,  $[Asc] = 1$  mM in [phosphate buffer] = 100 mM at pH 7.1. Scan rate =  $100$   $mV \cdot s^{-1}$ ; WE = Glassy carbon, Ref = SCE, CE = Pt wire.

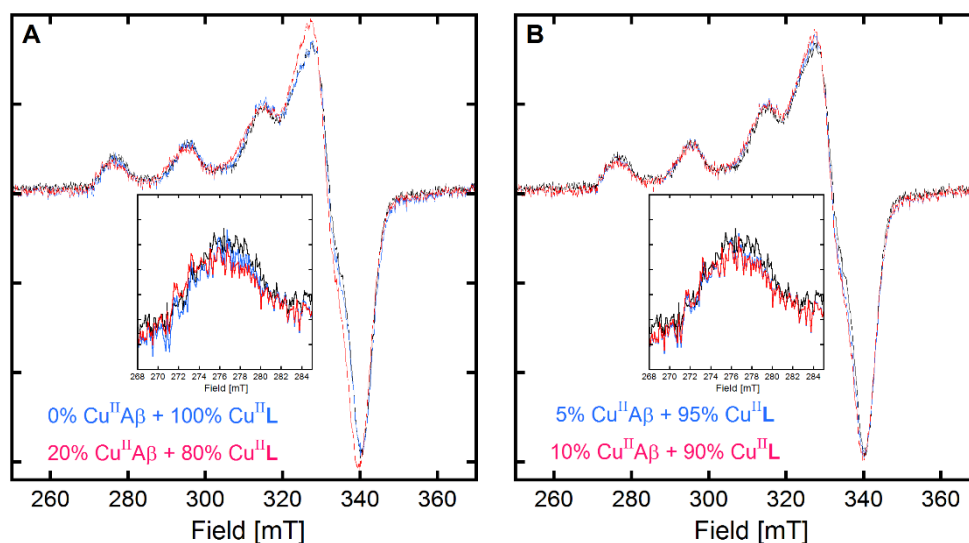


**Figure S6.** *Panel A.* EPR experiments of  $Cu^{II}A\beta_{1-16} + Cu^{II}L$  (black curve), linear combination: 0%  $Cu^{II}A\beta_{1-16} + 100\%$   $Cu^{II}L$  (blue curve), linear combination: 20%  $Cu^{II}A\beta_{1-16} + 80\%$   $Cu^{II}L$  (pink curve). The inset corresponds to a zoom of the first band. *Panel B.* EPR experiments of  $Cu^{II}A\beta_{1-16} + Cu^{II}L$  (black curve), linear combination: 5%  $Cu^{II}A\beta_{1-16} + 95\%$   $Cu^{II}L$  (blue curve), linear combination: 10%  $Cu^{II}A\beta_{1-16} + 90\%$   $Cu^{II}L$  (pink curve). The inset corresponds to a zoom of the first band.  $[L] = [A\beta_{1-16}] = [^{65}Cu^{II}] = 200$   $\mu M$ ,  $[HEPES] = 50$  mM, pH 7.1. 10% of glycerol was used as cryoprotectant.  $T = 110$  K.

Only insignificant difference can be observed in the reproduction of the experimental competition spectrum using 0 - 100 % ; 5 - 95 % and 10 % - 90 % as  $Cu^{II}A\beta_{1-16} - Cu^{II}L$  ratio. We thus propose that in the competition spectrum there is 5 % +/- 5% of  $Cu^{II}A\beta_{1-16}$ .

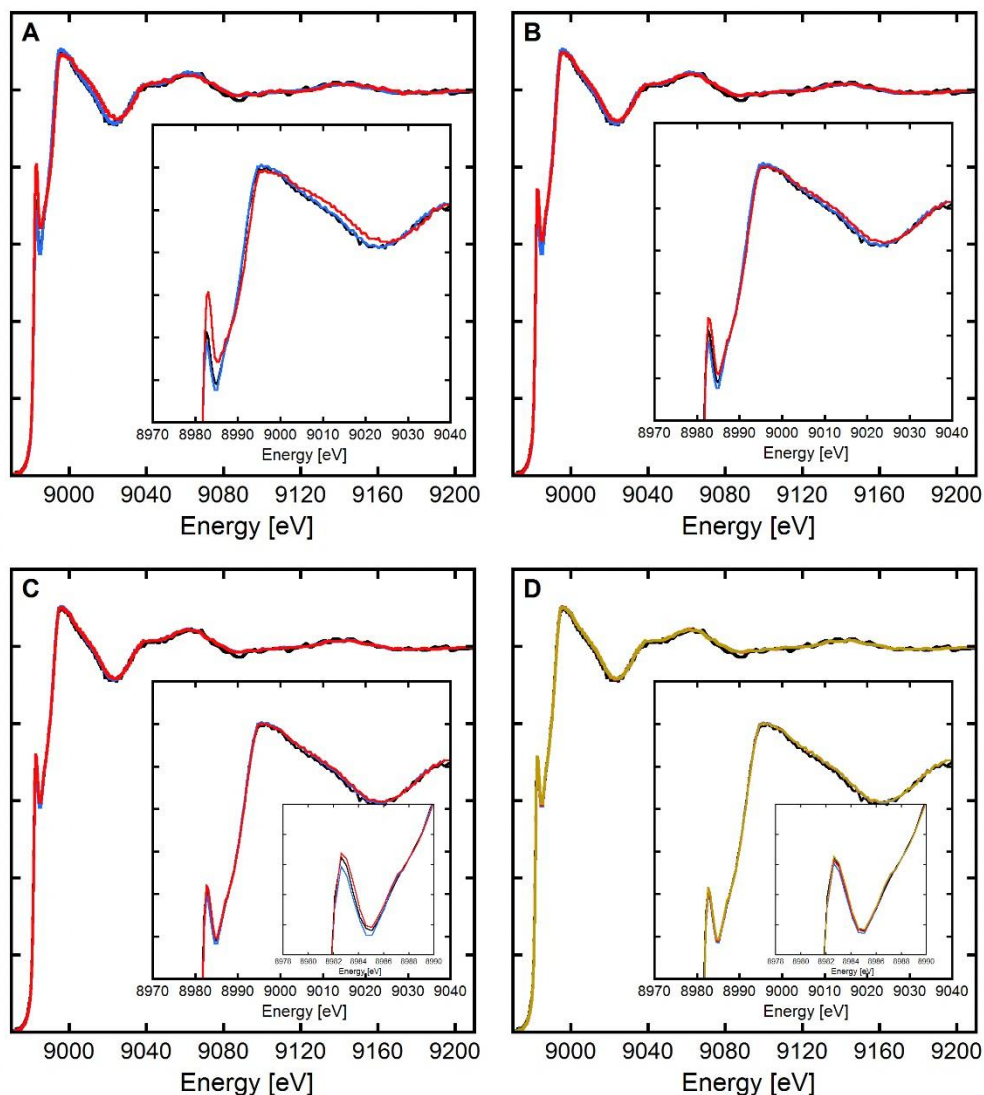


**Figure S7.** *Panel A.* XANES spectra of  $\text{Cu}^{\text{I}}\text{A}\beta_{1-16} + \text{Cu}^{\text{I}}\text{L}$  (black line), linear combination: 0%  $\text{Cu}^{\text{I}}\text{A}\beta_{1-16} + 100\%$   $\text{Cu}^{\text{I}}\text{L}$  (blue line), linear combination: 100%  $\text{Cu}^{\text{I}}\text{A}\beta_{1-16} + 0\%$   $\text{Cu}^{\text{I}}\text{L}$  (red line). *Panel B.* XANES spectra of  $\text{Cu}^{\text{I}}\text{A}\beta_{1-16} + \text{Cu}^{\text{I}}\text{L}$  (black line), linear combination: 0%  $\text{Cu}^{\text{I}}\text{A}\beta_{1-16} + 100\%$   $\text{Cu}^{\text{I}}\text{L}$  (blue line), linear combination: 50%  $\text{Cu}^{\text{I}}\text{A}\beta_{1-16} + 50\%$   $\text{Cu}^{\text{I}}\text{L}$  (red line). *Panel C.* XANES spectra of  $\text{Cu}^{\text{I}}\text{A}\beta_{1-16} + \text{Cu}^{\text{I}}\text{L}$  (black line), linear combination: 10%  $\text{Cu}^{\text{I}}\text{A}\beta_{1-16} + 90\%$   $\text{Cu}^{\text{I}}\text{L}$  (blue line), linear combination: 30%  $\text{Cu}^{\text{I}}\text{A}\beta_{1-16} + 70\%$   $\text{Cu}^{\text{I}}\text{L}$  (red line). *Panel D.* XANES spectra of  $\text{Cu}^{\text{I}}\text{A}\beta_{1-16} + \text{Cu}^{\text{I}}\text{L}$  (black line), linear combination: 15%  $\text{Cu}^{\text{I}}\text{A}\beta_{1-16} + 85\%$   $\text{Cu}^{\text{I}}\text{L}$  (blue line), linear combination: 20%  $\text{Cu}^{\text{I}}\text{A}\beta_{1-16} + 80\%$   $\text{Cu}^{\text{I}}\text{L}$  (red line), linear combination: 25%  $\text{Cu}^{\text{I}}\text{A}\beta_{1-16} + 75\%$   $\text{Cu}^{\text{I}}\text{L}$  (green line). The insets correspond to a zoom of the absorption.  $[\text{L}] = [\text{A}\beta_{1-16}] = 1.00 \text{ mM}$ ,  $[\text{Cu}^{\text{II}}] = 0.95 \text{ mM}$ ,  $[\text{dithionite}] = 10 \text{ mM}$ ,  $[\text{HEPES}] = 100 \text{ mM}$ , pH 7.1. 10% of glycerol was used as cryoprotectant.

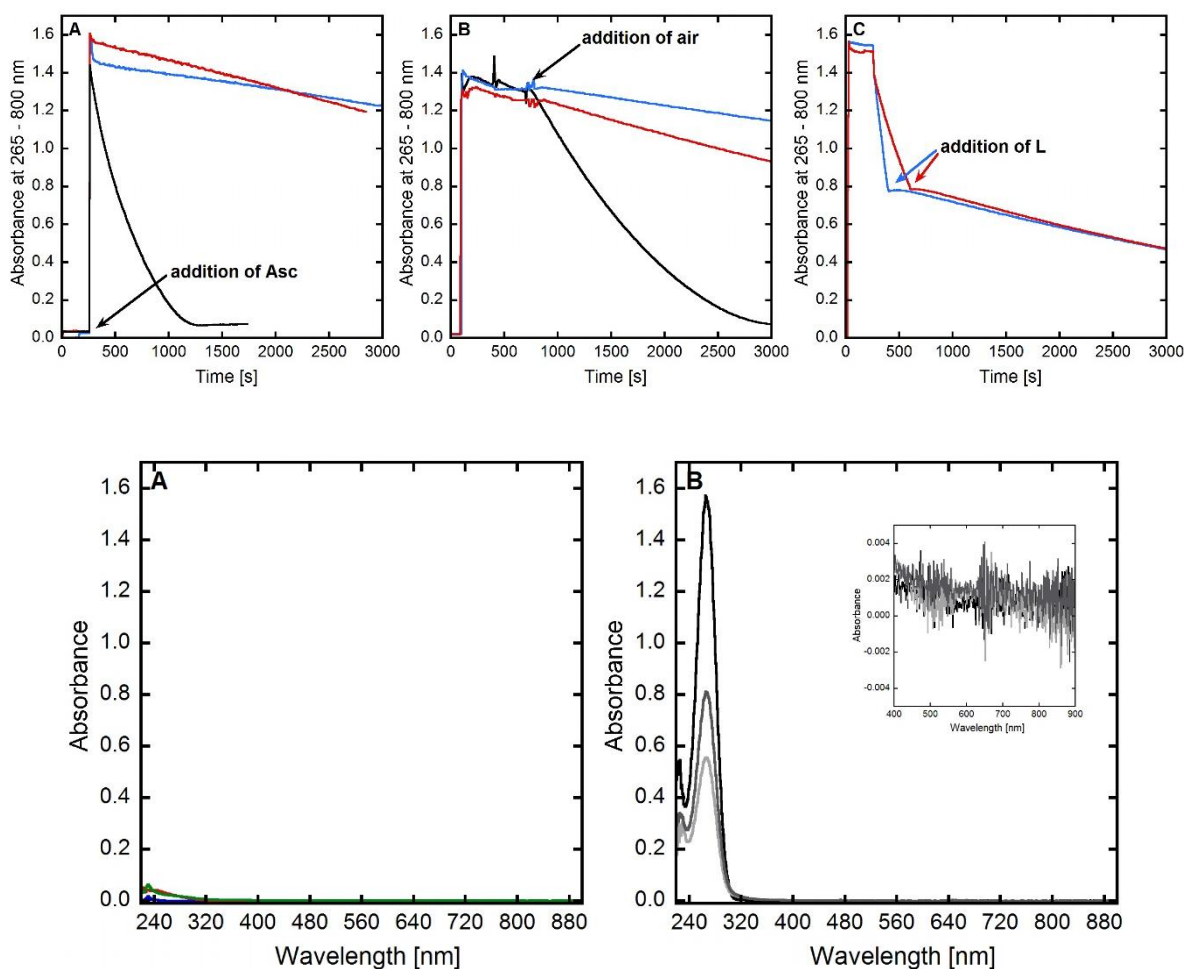


**Figure S8. Top:** Kinetics of ascorbate consumption, followed by UV-visible spectroscopy at 265 with subtraction of the background signal at 800 nm. *Panel A.*  $A\beta_{1-16} + Cu^{II} + Asc$  (black curve),  $L + Cu^{II} + Asc$  (blue curve),  $A\beta_{1-16} + Cu^{II} + L + Asc$  (red curve). *Panel B.*  $Cu^{II} + Asc + A\beta_{1-16} + air$  (black curve),  $Cu^{II} + Asc + L + air$  (blue curve),  $Cu^{II} + Asc + A\beta_{1-16} + L + air$  (red curve). *Panel C.*  $Asc + Cu^{II} + L$  (blue curve),  $Asc + A\beta_{1-16} + Cu^{II} + L$  (red curve).  $[L] = [A\beta_{1-16}] = 12 \mu M$ ,  $[Cu^{II}] = 10 \mu M$ ,  $[Asc] = 100 \mu M$ ,  $[HEPES] = 100 \text{ mM}$ ,  $pH 7.1$ . For the experiments from Panel B, all the solutions were deoxygenated by bubbling Argon and were added under a little overpressure of Argon in order to keep Cu under its +I oxidation state. **Bottom:** *Panel A.* UV-vis spectra of  $L$  (blue curve),  $L + Cu^{II}$  (red curve),  $L + Cu^I$  (green curve).  $[L] = 100 \mu M$ ,  $[Cu^{II}] = [Cu^I] = 100 \mu M$ ,  $[HEPES] = 100 \text{ mM}$ ,  $pH 7.1$ . To ease direct comparison, the absorbance intensity has been divided by a factor of ten since data were recorded at a ten-fold higher concentration to improve the signal over noise ratio. *Panel B.* Spectra corresponding to the experiment shown in Figure 7.  $Asc + A\beta_{40}$  (black curve),  $Asc + A\beta_{40} + Cu^{II}$  at 720 s, just before the addition of  $L$  (dark grey curve),  $Asc + A\beta_{40} + Cu^{II} + L$  at the end of the kinetic (light grey curve).  $[L] = [A\beta_{1-16}] = 12 \mu M$ ,  $[Cu^{II}] = 10 \mu M$ ,  $[Asc] = 100 \mu M$ ,  $[HEPES] = 100 \text{ mM}$ ,  $pH 7.1$ .

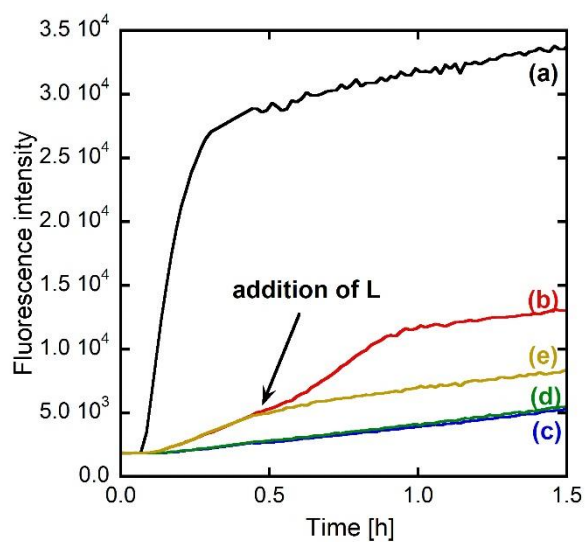


**Figure S9.** Fluorescence kinetics of CCA experiments of (a)  $\text{Cu}^{\text{II}} + \text{Asc}$ , (b)  $\text{A}\beta_{1-16} + \text{Cu}^{\text{II}} + \text{Asc}$ , (c)  $\text{L} + \text{Cu}^{\text{II}} + \text{Asc}$ , (d)  $\text{A}\beta_{1-16} + \text{Cu}^{\text{II}} + \text{L} + \text{Asc}$ , (e)  $\text{A}\beta_{1-16} + \text{Cu}^{\text{II}} + \text{Asc} + \text{L}$  at 20 min. Asc was added 5 min after the beginning of the measurement.  $[\text{L}] = [\text{A}\beta_{1-16}] = 12 \mu\text{M}$ ,  $[\text{Cu}^{\text{II}}] = 10 \mu\text{M}$ ,  $[\text{CCA}] = 500 \mu\text{M}$ ,  $[\text{Asc}] = 500 \mu\text{M}$ ,  $[\text{phosphate buffer}] = 50 \text{ mM}$ ,  $\text{pH } 7.1$ .



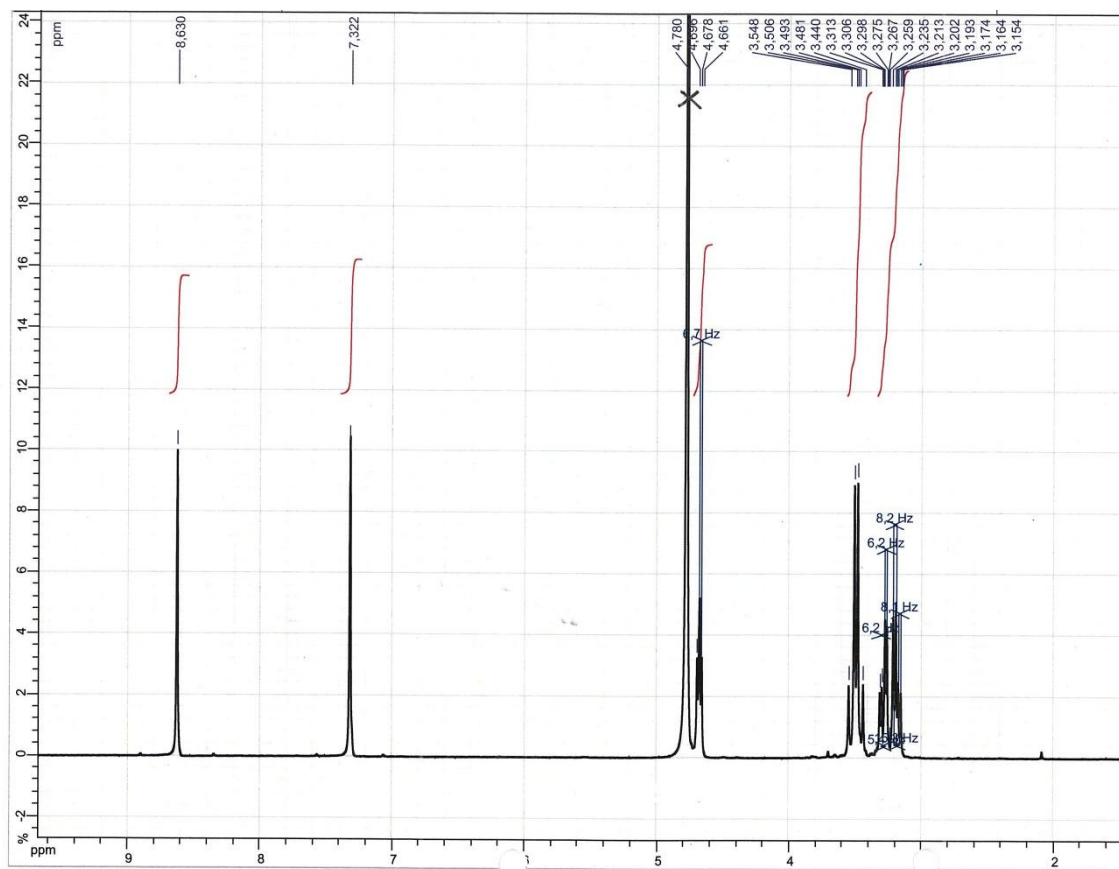
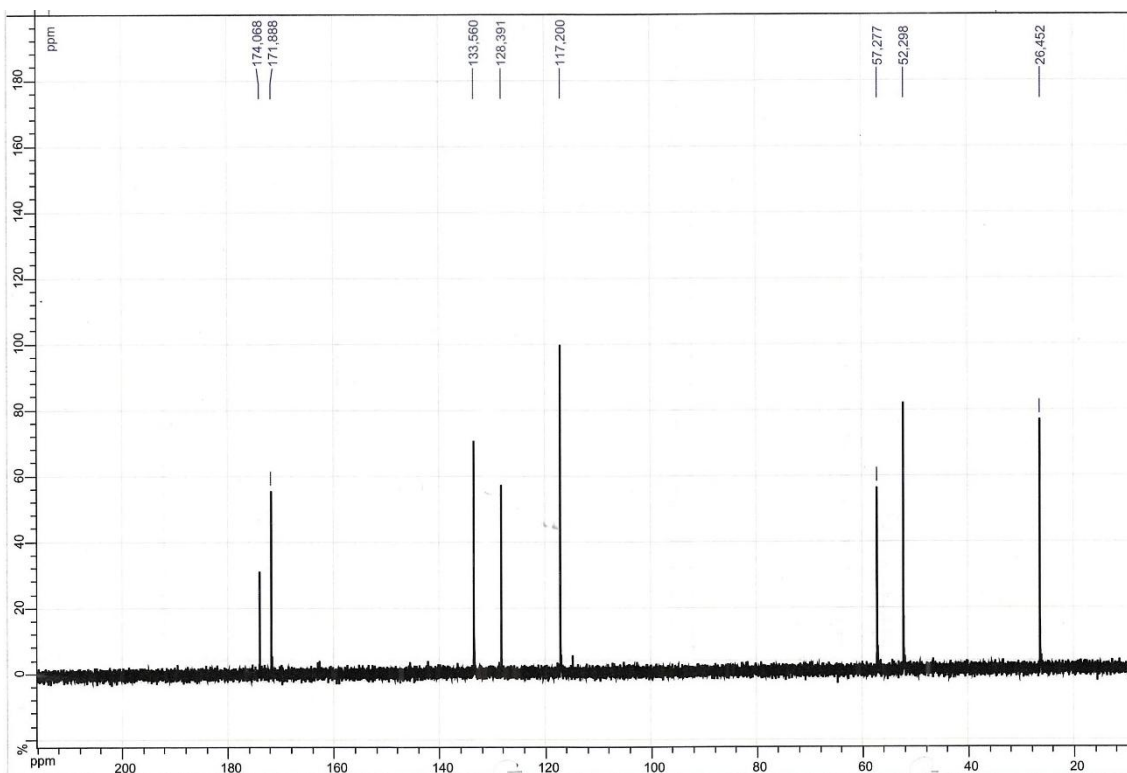


Figure S10. 400 MHz  $^1\text{H}$  NMR spectrum in  $\text{D}_2\text{O}$  at 300 K.



**Figure S11.** 100 MHz  $^{13}\text{C}$  NMR spectrum decoupled from  $^1\text{H}$  in  $\text{D}_2\text{O}$  at 300 K.